Free tropospheric ozone variability during NASA SEAC⁴RS (2013): Insights from ozonesondes, aircraft trace gas measurements and models

Zachary Fasnacht

Scholarly Paper

April 2016

Department of Atmospheric and Oceanic Science
University of Maryland

Research Advisor: Dr. Anne Thompson

Acknowledgements

I would like to thank Dr. Anne Thompson for all of her assistance and guidance as my advisor through my master's research. Additionally, I would like to thank Dr. Ryan Stauffer, Dr. Debra Kollonige, Dr. Ross Salawitch, Dr. Russell Dickerson, and Dr. Lesley Ott for all of their advice and guidance with my research. Finally, I greatly appreciate funding and support from NASA ACCDAM.

Abstract

The SEAC^{4}RS (Studies of Emissions and Atmospheric Composition, Clouds and Climate Coupling by Regional Surveys) field mission, based at Ellington Field (Houston) during August and September 2013, was a three-aircraft mission that conducted 57 flights to investigate the interplay of chemistry, clouds and aerosols with meteorological variations during the season of the North American Monsoon. An ozonesonde network (SEACIONS, Southeast America Consortium for Intensive Ozonesonde Network Study) operated at seven cities in the south central and western US during SEAC^{4}RS. One of the SEAC^{4}RS goals was to quantify influences on free tropospheric ozone (O_3), which include biomass burning, convective and advective redistribution of pollution, lightning, and stratosphere-troposphere exchange events (STE). Of the 21 DC-8 flights during SEAC^{4}RS, three cases exhibited elevated free tropospheric O_3 across a large geographical area. Using observations from soundings, aircraft and satellite, we found that these events displayed O_3 30-50% greater than background O_3 mid-troposphere O_3, in this case ~70 ppbv. Mixing line analysis, similar to Anderson et al. (2016) with tracers of water vapor (H_2O) and carbon monoxide (CO), suggest possible mixed STE and biomass burning influences. The STE segments of individual flights frequently corresponded to the presence of a stratospheric tracer in NASA's GEOS-5 atmospheric general circulation model as well as localized O_3 maxima in a simulation of CMAQ. Although CMAQ did not use active fire emissions, it captured the vertical structure of O_3 reasonably well in several cases.

I. Introduction

Tropospheric ozone (O_3) is a greenhouse gas (Shine K. 2001) and impacts air quality in the boundary layer (Unger et al 2006). Ozone absorbs longwave radiation in the troposphere, affecting the radiative balance of the atmosphere, with radiative forcing in the troposphere between 240-440mWm^{-2} (Stevenson et al. 2013). Ozone

in the boundary layer negatively affects air quality, causing difficulty with breathing and exasperating existing conditions like asthma and chronic obstructive pulmonary disease (Lippman M 1989, Holmen et al 1997).

A well-known source of O_3 in the troposphere is stratosphere-troposphere exchange (STE) (Danielsen 1968, Shapiro 1980, Holton et al. 1995, Parrish et al. 2000, Stohl et al. 2003, Cooper et al. 2004). A common mechanism that leads to STE in the United States is associated with tropopause folding behind frontal passages. Upper level convergence in the left entrance region of the jet streak along a cold front creates the downward motion that leads to lowering of air from the stratosphere into the troposphere; a tropopause fold forms behind the front. STE can transport high concentrations of O_3 into the troposphere, but very low concentrations of water vapor (H_2O) and carbon monoxide (CO). These layers of air are sometimes referred to as High Ozone Low Water Vapor (HOLW). Previous research showed surface O_3 enhancements of 10-20ppbv across the western United States during STE events (Lin et al. 2012). Thompson et al. (2004) and Thompson et al. (2007) analyzed STE in the free troposphere using ozonesondes across the eastern and southern United States, but further analysis is needed using more tracers of stratospheric air and analyzing boundary layer impacts.

Free tropospheric O_3 can also be elevated due to enhanced O_3 production from transported pollution and biomass burning. Biomass burning releases atmospheric trace gases from vegetation such as nitrogen oxides (NOx), CO, carbon dioxide (CO_2), and volatile organic compounds (VOCs) (Parrington et al. 2012). Tropospheric O_3 has been shown to form as a secondary product of the increased concentrations of trace gases from biomass burning (Oltmans et al. 2010). This leads to very polluted tropospheric profiles with elevated CO, hydrogen cyanide (HCN), O_3, and other pollutants (Marufu et al. 2000). The age of the smoke plays a crucial role on whether or not O_3 production has occurred, as fresh smoke emissions are too thick for radiation to be emitted through the top of the plume and reach the O_3 precursors in the plume (Jolleys et al. 2012). Tracers of biomass burning can be analyzed to

determine the age of a smoke plume as tracers such as formaldehyde (CH_2O) and ethene (C_2H_4) have a short lifetime of less than a day, while HCN has a lifetime of a few months in the troposphere (Alvarado et al. 2010).

The NASA SEAC^{4}RS campaign had several goals, including analyzing the redistribution of pollutants in deep convection, determining the impact of aerosol feedbacks on the atmospheric heat budget, and serving as validation for future satellite missions (Toon et al. 2016). The campaign, which was based in Houston, TX, occurred in August and September of 2013 over a large area of the United States, stretching from the northern Plains down to the Southern and Southeast United States. A network of ozonesonde launches Southeast America Consortium for Intensive Ozonesonde Network Study (SEACIONS) coincided with the NASA SEAC4RS campaign.

We analyze three enhanced tropospheric O_3 events (19 August, 21 September, and 23 September) to see if we can discriminate the various influences. A variety of atmospheric measurements from the DC-8 aircraft during the NASA SEAC^{4}RS field campaign allow for a thorough analysis of these events and their impact on tropospheric O_3. In section 2, we discuss the data used including aircraft and ozonesonde measurements, model output, and the methodology of using mixing line analysis. In section 3, we present results from our case studies during the SEAC^{4}RS field campaign.

II. Methods

NASA SEAC^{4}RS Observations

NASA's DC-8 aircraft flew a variety of flight paths on 21 days and the ER-2 flew on 23 days during August and September 2013. The DC-8 flights took off from Ellington, TX and sampled air from the planetary boundary layer (~1-2km) through

the upper troposphere (~12km) with in-situ observations as well as remotely sensed LiDAR measurements. The ER-2 flights also took off from Ellington, TX but sampled air throughout the stratosphere.

Instrumentation used for measurements from the DC-8 and ER-2 and uncertainties for each instrument shown in Table 1. Observations from the DC-8 aircraft of O_3, CO, and H_2O were used as stratospheric tracers, while O_3, CO, CH_2O, HCN, and C_2H_4 were used as biomass burning tracers. Ozone was measured with a nitric oxide-induced chemiluminescence instrument with an uncertainty of 0.3ppbv as used by Ryerson et al. (2003). As in previous research performed during the DC3 field campaign investigating UT/LS exchange, we used CO observations from the in-situ diode laser spectrometer known as DACOM, which has an uncertainty of ~1.4ppbv (Sachse et al. 1987, Schroeder et al. 2014). Additional measurements of H_2O were selected from the ER-2 to determine the background stratospheric H_2O for use in the mixing line analysis (most of the ER-2 flights were well into the stratosphere).

Species	Aircraft	Instrument	Uncertainty	Reference
O_3	DC-8	Nitric Oxide-Induced Chemiluminescence	0.3ppbv	Ryerson et al 2003
CO	DC-8	Diode Laser Spectrometer	1.4ppbv	Sachse et al 1987; Schroeder et al 2014
H_2O	DC-8	Diode Laser Hygrometer	0.75ppmv	Vay et al 200; Podolske et al 2003
CH_2O	DC-8	Compact Atmospheric Multispecies Spectrometer	45pptv	Weibring et al 2010
HCN	DC-8	Chemical Ionization Mass Spectrometer	36pptv	Viggiano et al 2003
C_2H_4	DC-8	Chemical Ionization Mass Spectrometer	0.7ppbv	Washenfelder et al 2010
H_2O	ER-2	Laser Hygrometer	0.05ppmv	May R. 1998

Table 1: Instrument and given uncertainty for each measurement used

Profiles of O_3 are analyzed using ozonesonde measurements to identify possible stratospheric intrusion cases and evaluate model results. Electrochemical concentration cell ozonesondes were used to perform measurements; measurement method and uncertainties are discussed in Thompson et al. (2007). Ozonesondes were used to measure O_3 from the surface to ~20km. The launches took place at

eight sites across the United States during the NASA SEAC^{4}RS campaign: Idabel, OK; Houston, TX; Ellington, TX; Tallahassee, FL; Huntsville, AL; Socorro, NM; Boulder, CO; St. Louis, MO.

Ground based measurements from Penn States Nittany Atmospheric Trailer & Integrated Validation Experiment (NATIVE) trailer at Smith Point, TX are used to analyze impact of tropospheric O_3 enhancements on surface air quality. The NATIVE trailer measured O_3 using a UV-absorption spectrometer, CO using an infrared absorption spectrometer, and relative humidity using a standard R.M. Young hygrometer; details on measurements and uncertainties discussed by Martins et al. (2012).

Mixing Line Analysis

In this work, we employ a mixing line analysis similar to that performed in Anderson et al. (2015) to determine the prevalence of stratospheric air in the troposphere for our case studies. The mixing line analysis is performed using H_2O and CO as stratospheric tracers from aircraft measurements, as the stratosphere has very low concentrations of each. The H_2O and CO concentrations were compared with their typical background values. The first step is to calculate the estimated percentage of stratospheric air by comparing the water vapor mixing ratio to its background values as shown in equation 1, where H_2O_{obs} is the observed H_2O for the observation being analyzed, H_2O_{strat} is the background stratospheric H_2O, $H_2O_{TROP(z)}$ is the background troposphere H_2O, and f_{strat} is the percentage of stratospheric air in the observed sample of air.

$$H_2O_{obs} = f_{strat}H_2O_{strat} + (1-f_{strat})H_2O_{TROP(z)} \qquad \text{(eq. 1)}$$

The background value of stratospheric water vapor mixing ratio was determined to be 6ppmv from the ER-2 measurements. The background tropospheric water vapor

mixing ratio was estimated for each 1km layer. Determining the background tropospheric H_2O was highly complex and required analysis of the distribution of water vapor mixing ratio in each layer throughout the campaign. Since the campaign occurred across a large geographic region we analyzed the background values for the region within 32N-42N and 80W-105W for altitudes between 0-12km. Despite removing any possible stratospheric cases from this analysis, most layers exhibited a bimodal or trimodal distribution due to the presence of convection or regions of surface high pressure. Given the multiple modes, the background value was selected as the median of the lowest value mode. Air drier than the background value indicates air of stratospheric origin. After calculating f_{strat}, the expected mixing ratio of CO from the stratosphere was calculated using equation 2, where $CO_{strat\ inferred}$ is the calculated amount of CO originating from the stratosphere, CO_{obs} is the concentration of CO being observed, and CO_{TROP} is the background tropospheric CO.

$$CO_{Strat\ Inferred} = [CO_{obs} - (1\text{-}f_{strat})CO_{TROP}]/f_{strat} \qquad \text{(eq. 2)}$$

Here f_{strat} was used from the calculation in equation 1 and CO_{TROP} was again determined by analyzing the distribution of CO in the troposphere for 1km bins. Unlike H_2O this analysis showed only unimodal distributions, so the median of these CO distributions was accepted as the background value.

Models

NASA's GEOS-5 is an atmospheric general circulation model with 72 vertical layers and a horizontal resolution of 50km. Stratospheric tracers used here are transported by GEOS-5 based on initially setting the troposphere to 0 and the stratosphere to 1. Once the model is run, mixing occurs between the troposphere and stratosphere altering these initial values. Further details on the model set-up and parameters can be found in Ott et al (2016). We also used the EPA's regional air quality model CMAQ for these cases to determine whether it could correctly

represent elevated O_3 events in the troposphere. For this study, CMAQ was analyzed at a horizontal resolution of 36km and a vertical resolution of 45 pressure levels. Biomass burning emissions were not included in the CMAQ model simulation. A similar model set up for CMAQ can be found in Canty et al (2015).

NOAA Hysplit back trajectories can be used to determine the long-range transport that may affect certain regions. Anderson et al. (2015) uses back trajectories to analyze the origin of HOLW layers in the tropical west Pacific. We use the Global Data Assimilation System (GDAS) meteorology at a resolution of 0.5 degree for our trajectories, run back in time for two weeks from initialization.

II. Results

August 19, 2013

Meteorological Conditions

On the days leading up to this event, a large high-pressure system affected much of the nation. Temperatures across the central United States were in the 80s, but dew points were very low in the 20s-30s leading to prime fire conditions. Wildfires had been burning in Idaho, Colorado, and Montana since 9 August. On the 16th, fire coverage intensified with many significant fires across the northern Rockies and pyrocumulus clouds in Montana. As the fires continued to burn, smoke continued to spread east across the central Plains through 20 August as shown in MODIS satellite imagery in Figures 2a and 2b.

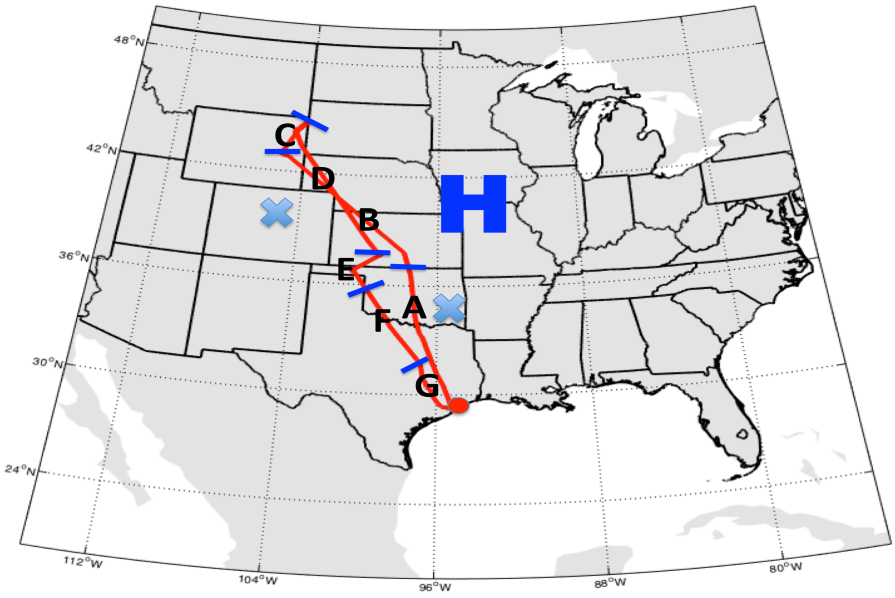

Figure 1: Map of the DC-8 flight path (red line) on 19 August with separate legs of flight denoted by capital letters. Blue X denotes location of ozonesonde launches that are analyzed and red dot denotes location of aircraft base.

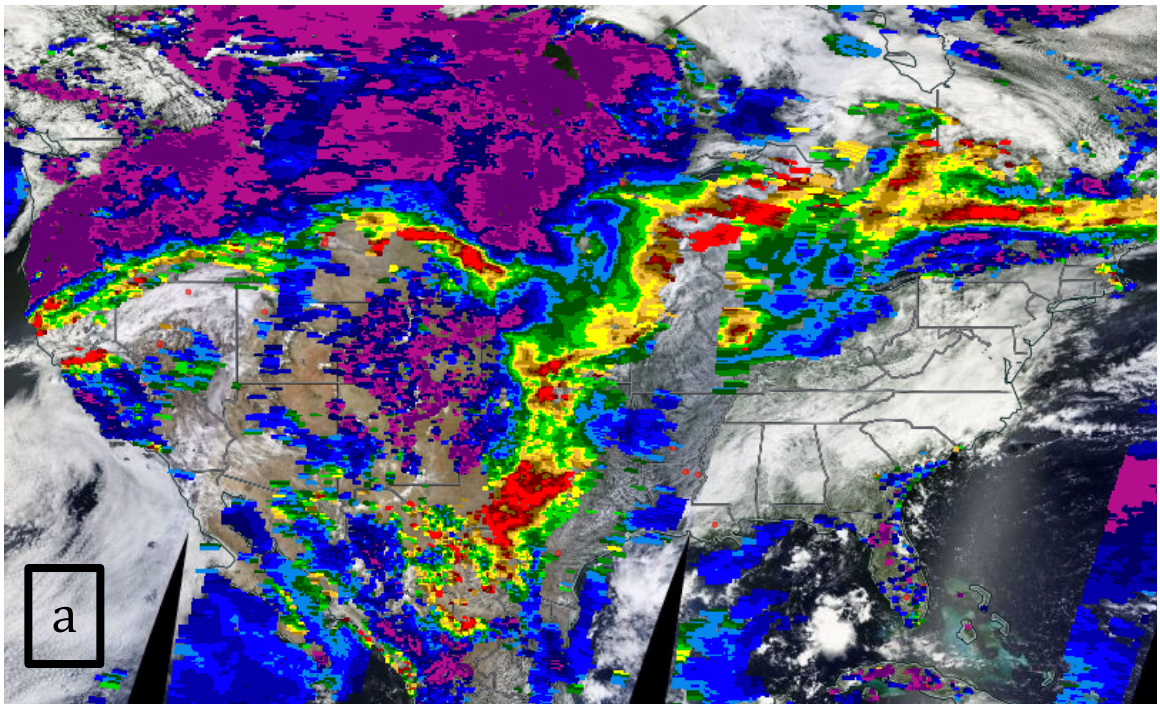

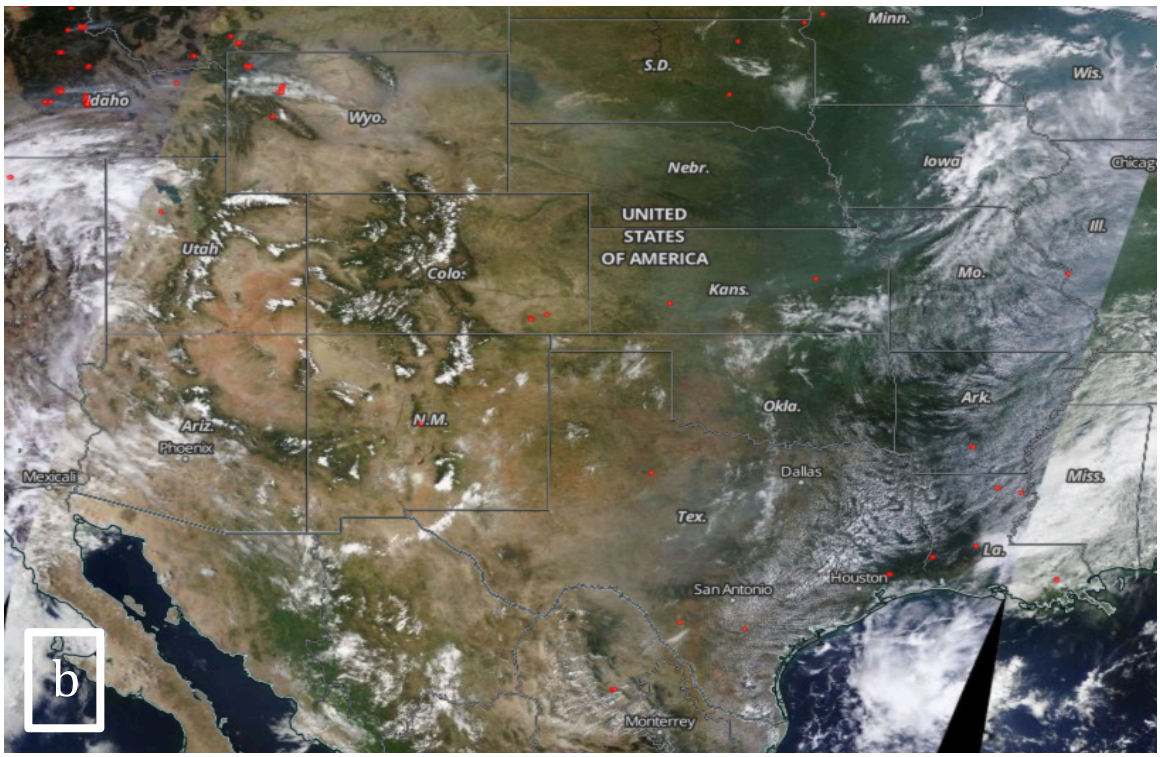

Figure 2: a) MODIS aerosol optical depth (AOD) across the United States on 19 August 2013. Hotter colors represent higher AOD values; b) MODIS visible satellite imagery with red dots representing locations of active fires.

Observations

On 19 August, the DC-8 flew directly through smoke that had spread through the central Plains. Throughout the flight, smoke plumes appear to vary in age based on satellite trends and observations, with differing impacts on tropospheric O_3 depending on the plume age. The early portion of the flight (Figure 1 Region A) experienced some smoke as the aircraft was flying towards the large region of thicker smoke shown by MODIS in Figure 2a. In this region, both CO and O_3 were near background values of ~75ppbv, whereas HCN was around 450pptv.

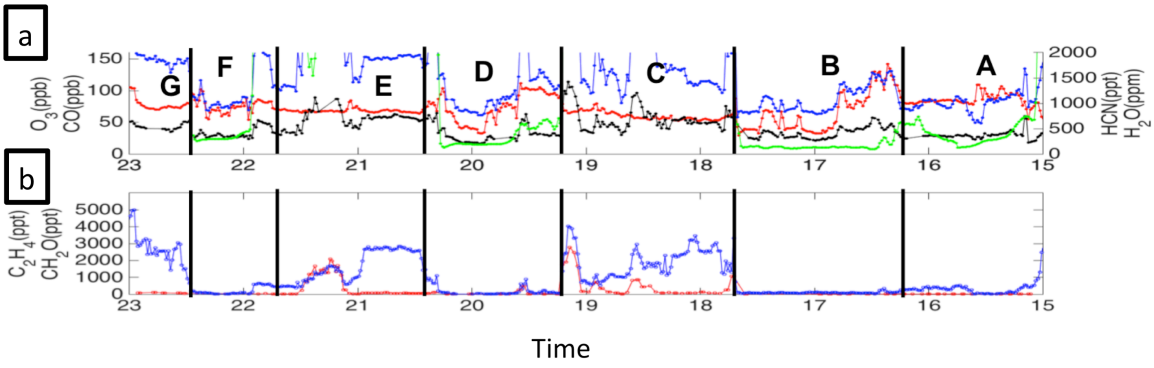

Figure 3: Image shows observations and model simulations on 19 August 2013. a) In-situ aircraft observations of O_3 (red), CO (blue), H_2O (green), and HCN (black). b) In-situ aircraft observations of C_2H_4 (blue) and CH_2O (red)

The DC-8 continued its course to the west, flying into the large region of smoke spread across Oklahoma, Kansas, and Nebraska, as shown by MODIS in Figure 2a. A tight correlation was observed in this region (Figure 3a region B) between O_3 and CO (r^2 of 0.95) as well as O_3 and HCN (r^2 of 0.88) with each enhancement well above background levels. Ethene and CH_2O showed no significant increase in this region due to their short lifetimes of less than a day. This smoke plume experienced very high O_3 above 100ppbv due to the photochemical production from biomass burning emissions. The enhanced production of O_3 in this region is faster than research has shown for other regions such as Africa, Southeast Asia, and Canada. This may be due to the background levels of O_3 precursors being higher due to pollution mixing or elevated O_3 from vertical transport in the UT/LS.

As the DC-8 continued flying northwest, it began moving into a region of active burning and fresh smoke plumes. This portion of the flight, shown in Figures 3a and 3b (section C), measured tight correlations between CO, HCN, CH_2O, and C_2H_4 suggesting the smoke plumes were relatively fresh. Ozone shows no enhancement in this region, as there was a short time between release of hydrocarbons and measurements with not enough time for enhanced photochemical production of O_3.

The DC-8 turned back towards Texas flying through the same aged smoke plume measured in leg B of the flight. As with the earlier leg B, this flight portion (Figure 3a section D) measured elevated CO, O_3, and HCN that were well above background values. No significant enhancements of CH_2O or C_2H_4 were measured. The O_3 in this portion was again elevated by photochemical O_3 production from the biomass burning with measurements around 100ppbv.

On the way back to Ellington, TX the DC-8 flew through the Texas panhandle; first measuring polluted boundary layer air and again measuring localized active burning. In this region (Figures 3a and 3b section E) enhanced C_2H_4 and CH_2O were measured along with elevated CO and HCN. As with the fresh smoke in Wyoming, these measurements suggest very little variability in O_3 as it stayed near its background value of ~75ppbv. Once leaving the region near the Texas panhandle, the DC-8 flew back out of the smoke plume in eastern Texas measuring typical background tropospheric air with CO and O_3 around ~75ppbv while HCN dropped to ~400pptv in regions F & G on Figure 3a.

Models

The GEOS-5 stratospheric tracer for 19 August shows very small stratospheric influence as shown in Figure 4b, which agrees with observations as the high O_3 appears to be mostly of biomass burning origins. There were several regions with small stratospheric influence in the GEOS-5 model, such as in Figure 4a around 300-400mb. Since this CMAQ version was not initialized with fire emissions, it does not reproduce the high values of O_3 associated with smoke plumes where DIAL O_3 and in-situ observations measured O_3 ~70-90ppbv (around 1920UTC on Figures 3a and 4a). CMAQ, however, does seem to perform well in modeling the background O_3. Figure 5 shows CMAQ O_3 profiles have similar shapes ozonesonde profiles at Idabel,

OK and Boulder, TX, but misses the smaller scale vertical variability associated with the individual smoke plume layers.

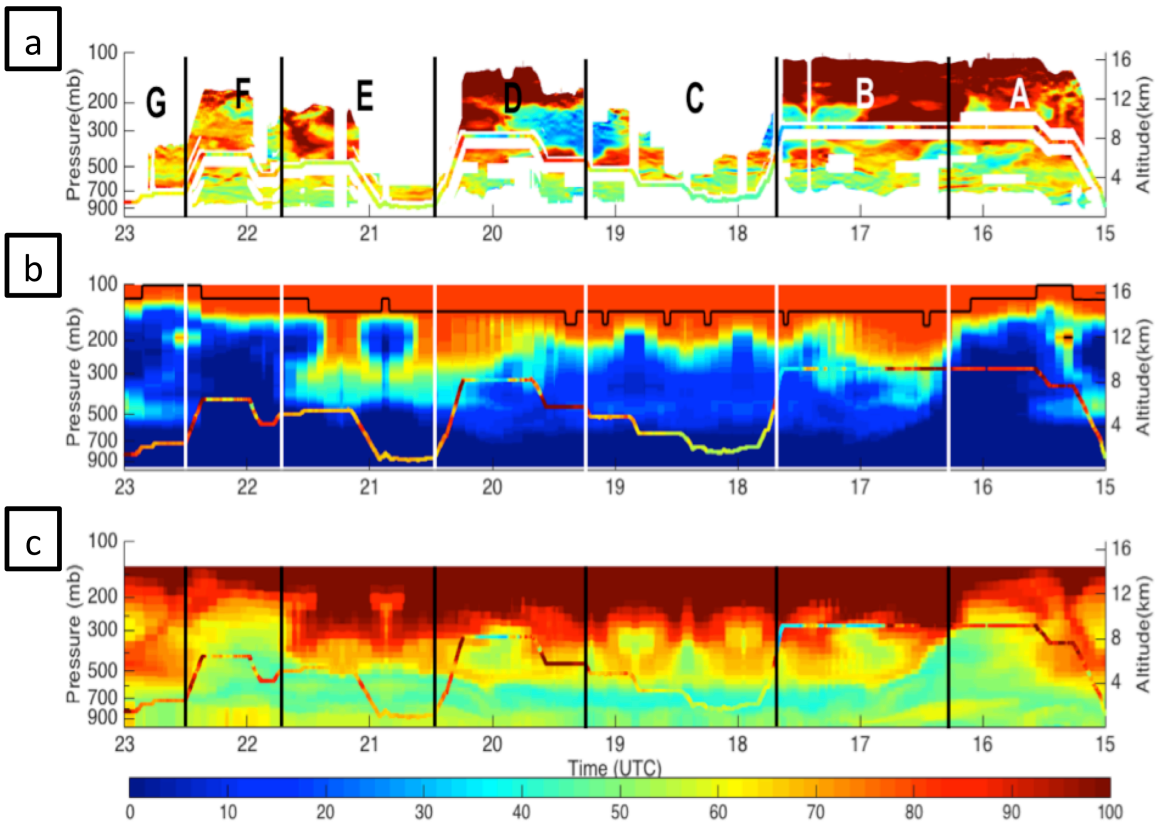

Figure 4: LiDAR observations and model simulations for 19 August 2013. a) DIAL LiDAR O_3 profile; b) GEOS-5 stratospheric tracer with in-situ aircraft observations overlaid; c) CMAQ O_3 with in-situ aircraft observations overlaid

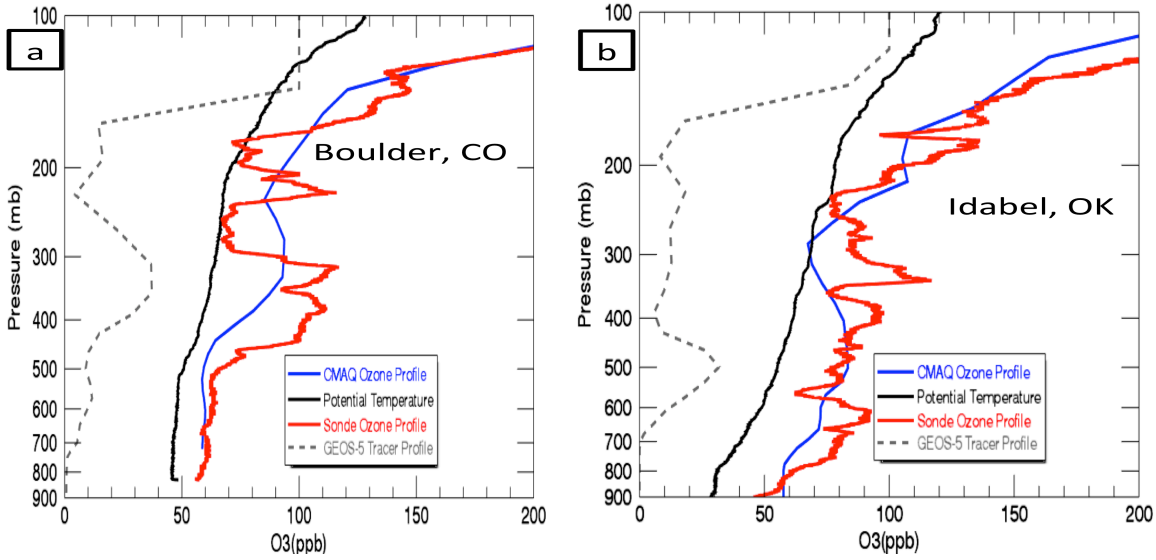

Figure 5: Profiles on 19 August 2013 from Boulder, CO at 18UTC (a) and Idabel, OK at 18UTC (b) with ozonesonde observed O_3 (in red), CMAQ modeled O_3 (in blue), GEOS-5 stratospheric tracer (in gray), and ozonesonde observed potential temperature (in black).

Biomass burning in Montana and Wyoming spread plumes of smoke across much of the central United States within days. Within as many as three days enhanced production of O_3 was measured within the plumes due to elevated concentrations of O_3 precursors from the plumes of smoke. Aircraft measurements within the smoke plumes measured O_3 of 100-120ppbv three days after biomass burning.

September 21, 2013

Meteorological Conditions

Days prior to the intrusion event on 21 September, a 1024mb a high-pressure system resided in the eastern United States. High pressure led to minimal precipitation across the southeast United States with the exception being along the coastal regions of the Gulf of Mexico where summer thunderstorms developed. By

0900 UTC on 20 September, low pressure was moving into central Ontario with a cold front stretching southward through central Missouri, central Oklahoma, and northern Texas. The DC-8 flew a flight path through the front on the 21st, as shown on Figure 6, encountering tropopause folds in central Tennessee and central Louisiana. The front continued to slowly push east before finally exiting the east coast of the United States around 22 September at 1200 UTC. A line of thunderstorms stretched along the entirety of this front, with some severe weather including strong winds and hail in the upper midwest on 19 September. Significant rainfall amounts were also experienced as some areas in the south received over 150mm of rain from this frontal passage.

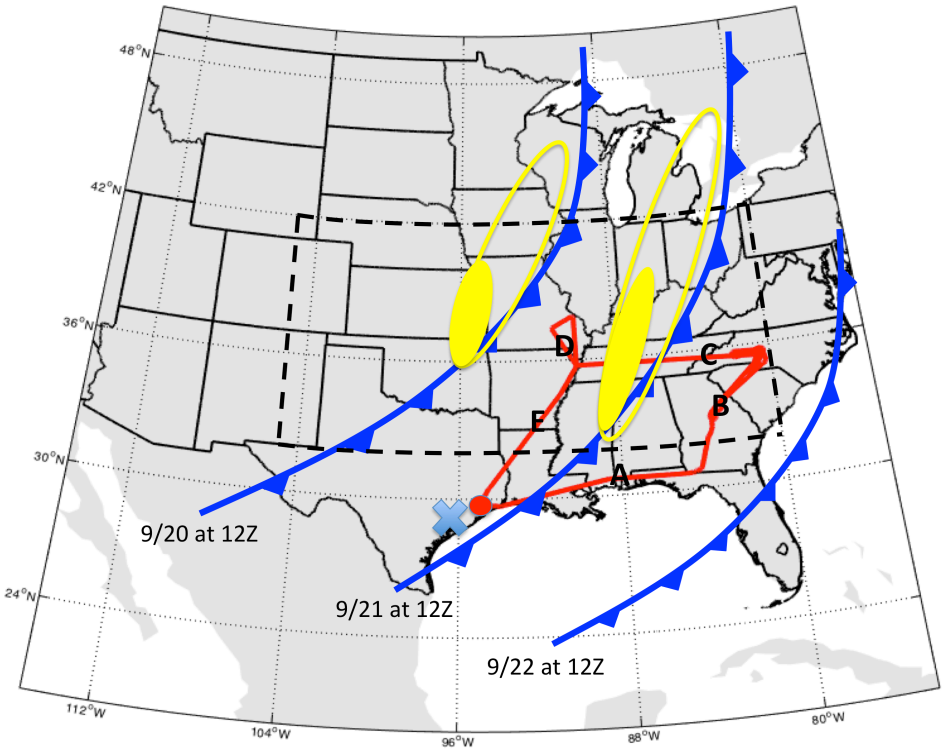

Figure 6: Map shows location of the cold front as it pushes through the southeast United States and flight path of DC-8 on 21 September 2013 in red line with letters representing different legs of the flight. Red dot is location where flight originated and blue x is site of Houston ozonesonde launches. Yellow circle represents region of jet streak with inner region representing area where stratospheric intrusion is likely.

Aircraft Observations/Mixing Line Analysis

On 21 September, the DC-8 aircraft sampled air on both sides of a cold front in the southeast United States as shown in Figure 6. Early in the flight (section A on Figure 7a from 1820UTC-1940UTC) the aircraft sampled prefrontal boundary layer air exhibiting CO around 120-140ppbv and H_2O mixing ratio over 20,000ppmv. The aircraft then sampled portions of the mid-troposphere ahead of the cold front from 1940UTC-2240UTC(leg B on Figure 7a), where CO and H_2O mixing ratio drop significantly but remained above background due to lofting of surface pollutants ahead of the front.

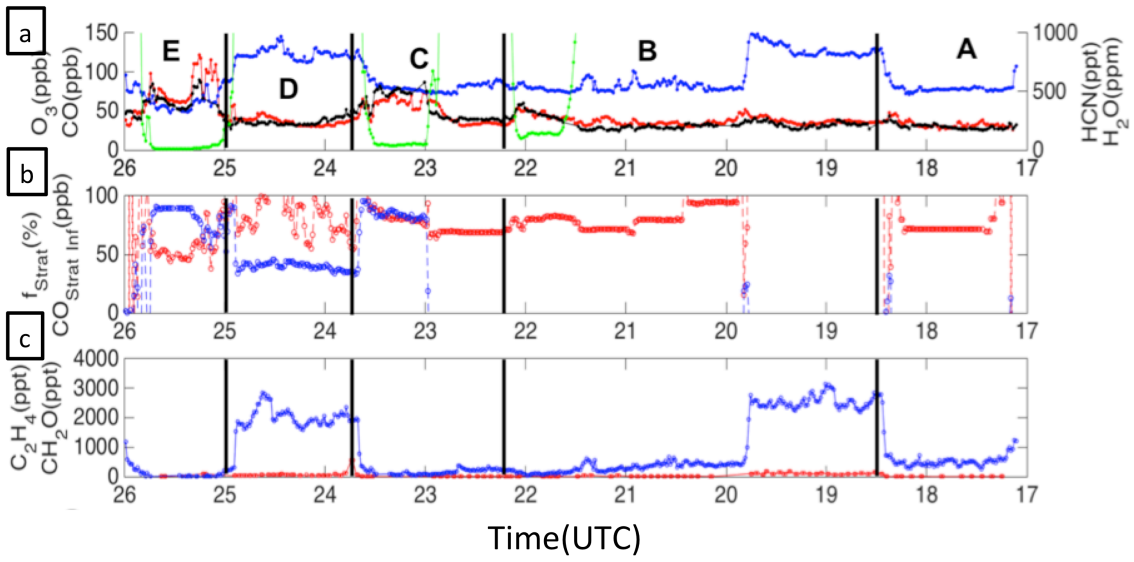

Figure 7: In-situ observations and model simulations on 21 September 2013. a) In-situ aircraft observations of O_3 (red), CO (blue), H_2O (green), and HCN (black); b) Mixing line analysis showing f_{strat}(in blue) and $CO_{Strat\ Inf}$(in red) c) In-situ aircraft observations of C_2H_4 (blue) and CH_2O (red)

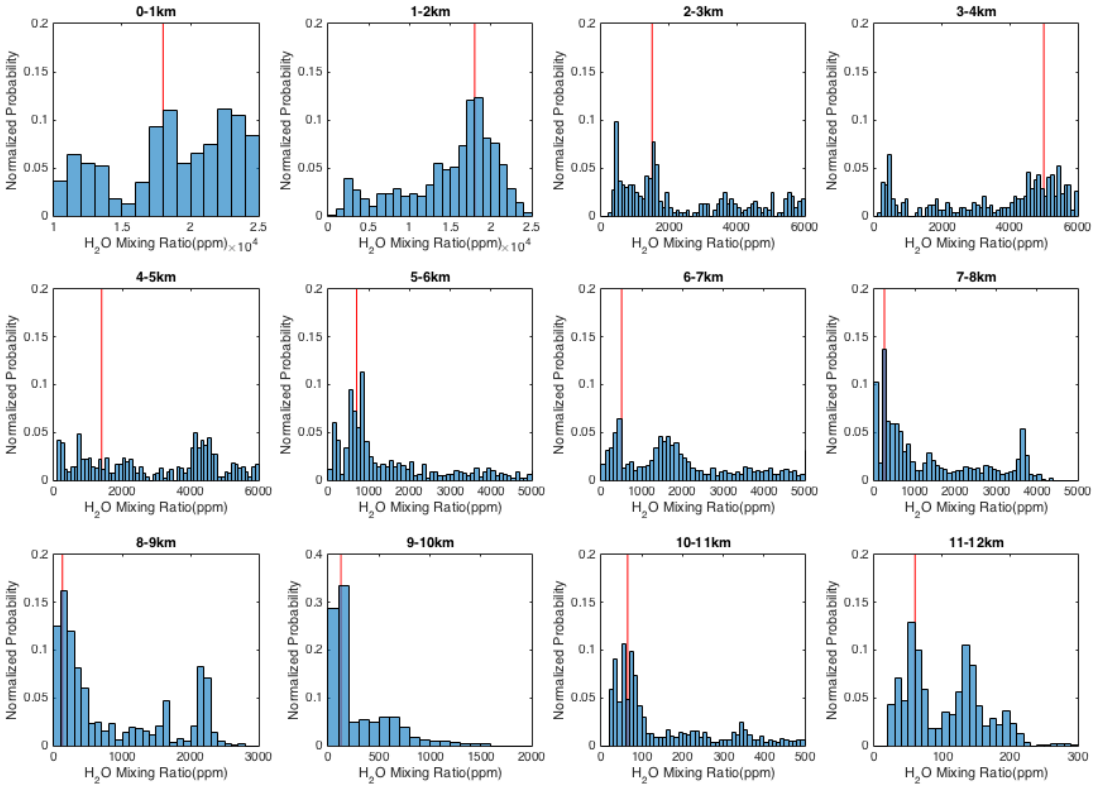

Figure 8: Histograms of H_2O for each 1km level from the DC-8 aircraft measurements showing the varying distributions in H_2O for the campaign. Red line is background H_2O chosen for each 1km bin.

Halfway through the flight (~2300UTC) the aircraft crossed the cold front for the first time in the mid troposphere at around 400mb. In-situ measurements in this region, shown in Figure 7a, signify a HOLW layer at around 400mb with O_3 ~60ppbv and H_2O ~50ppmv. A similar layer was measured around 2500UTC with O_3 ~90ppbv and H_2O ~20ppmv. In both of these layers CO was constant, but HCN measurements increased to around 500-600pptv and were highly correlated with O_3 measurements (r^2 of 0.65 for O_3 & HCN between 2300UTC-2340UTC and 0.89 for the layer measured from 2500UTC-2540UTC). As shown in Figure 7c, concentrations of C_2H_4 and CH_2O in these HOLW regions remained low. Since O_3 and HCN were correlated but C_2H_4 and CH_2O were low, this air likely had an aged biomass-burning component.

A mixing line analysis was performed for the in-situ measurements to determine the impact of stratospheric air in these regions. Background tropospheric H_2O was found to be ~125ppmv in the first HOLW region and ~60ppmv in the second HOLW region as shown in Figure 8. Both layers show a large percentage of stratospheric air around 90% (Figure 7b) which is consistent with the very dry air of ~20ppmv and high O_3 of ~100ppbv measured. The inferred stratospheric CO was 50-90ppbv, well above stratospheric background values, meaning some mixing with tropospheric air must have occurred as the stratospheric air moved into the troposphere.

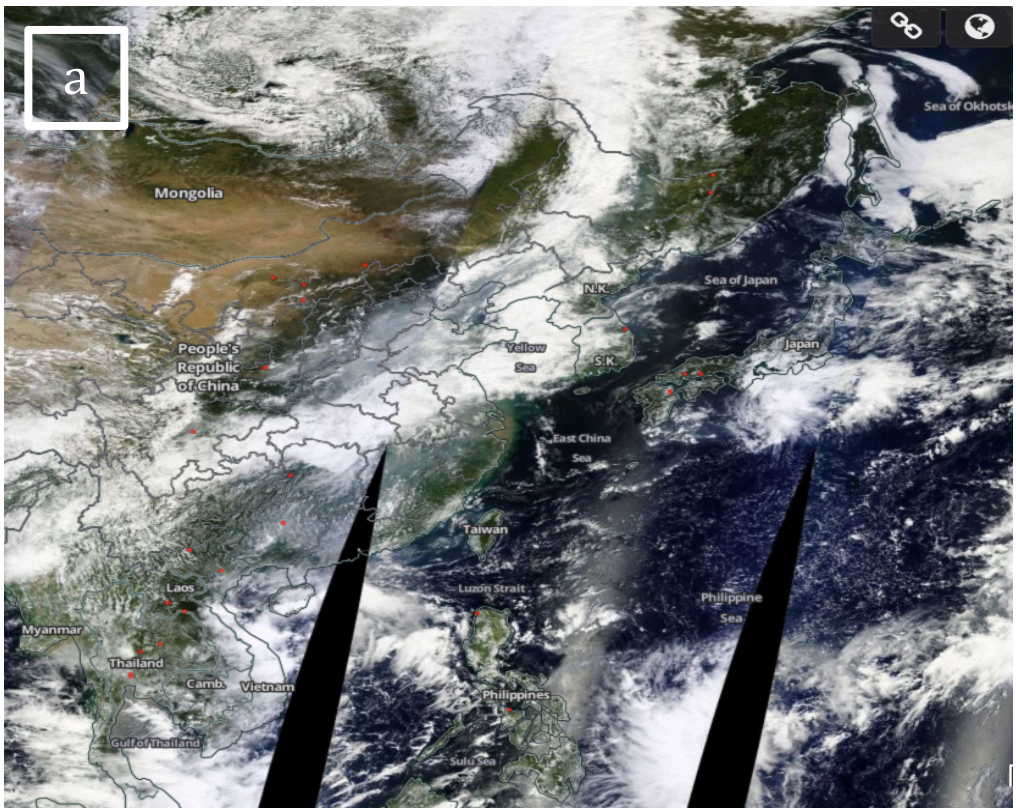

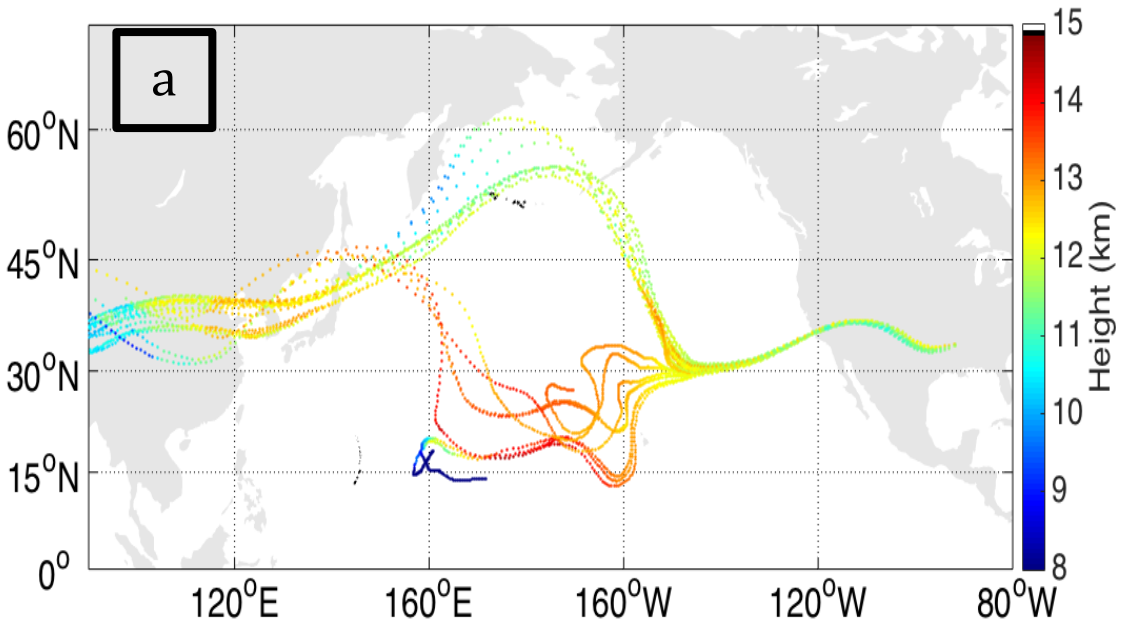

Figure 9: Satellite observations and model back trajectories for HOLW layer. a) MODIS visible satellite imagery for 10 September 2013 with red circles representing locations of active burning; b) NOAA Hysplit back trajectories initialized at 0015UTC on 22 September 2013 for 33.64N, -91.71W at 200mb.

While there was no burning occurring in the continental United States or Canada during this time period, there was widespread burning in eastern China as shown in Figure 9a with smoke spread across much of eastern China on 10 September 2013. NOAA HYSPLIT back trajectory ensembles (Figure 9b) were initialized on 22 September 2013 when the aircraft was located over Arkansas. The back trajectories showed the air in the HOLW region originating from the same region in eastern China where biomass burning was widespread. Given the back trajectories and in-situ observations this air likely contained air transported from regions of biomass burning in eastern China.

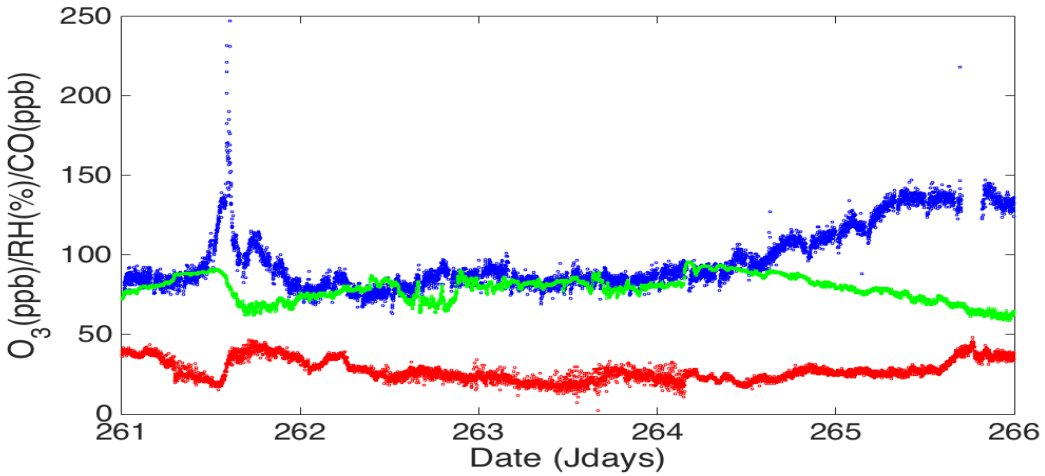

Figure 10: NATIVE ground observations for 18-23 September 2013 with O_3 (red), CO (blue), and RH (green)

Ground observations from the NATIVE trailer at Smith Point, TX shown in Figure 10, show no measurements resembling a HOLW layer as seen in the mid-troposphere following the intrusion on 21 September 2013 (Julian Day 264). The measurements of O_3 remain constant while CO increases later on 21 September. These measurements show that the air from the stratospheric intrusion did not reach the surface.

GEOS-5/CMAQ Model Simulations

When comparing GEOS-5 and CMAQ model simulations to the DIAL observations, the models generally reproduced the structure of elevated O_3. CMAQ performed well with some fine scale features as it has the two separate elevated O_3 layers that are shown in DIAL around 2500-2600UTC in the upper troposphere.

Unlike the structure of the elevated O_3, CMAQ incorrectly modeled the magnitude of O_3 as the intrusion is modeled to be well over 100ppbv (Figure 11c), while the DIAL observations show very few measurements of O_3 over 100pb (Figure 11a). The

background tropospheric O_3 was also modeled too high as CMAQ simulated widespread O_3 of 40-50ppbv but the DIAL measurements were only 20-40ppbv.

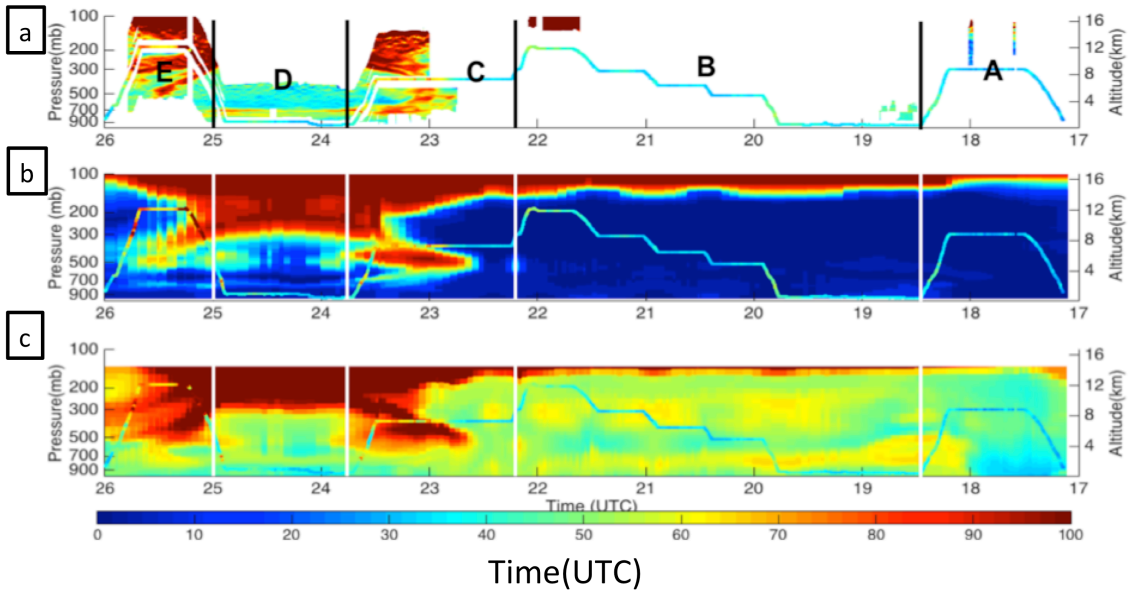

Figure 11: LiDAR observations and model simulations with in-situ aircraft profiles overlaid in each profile for 21 September 2013. a) DIAL LiDAR O3 profile; b) GEOS-5 stratospheric tracer profile; c) CMAQ O_3 profile

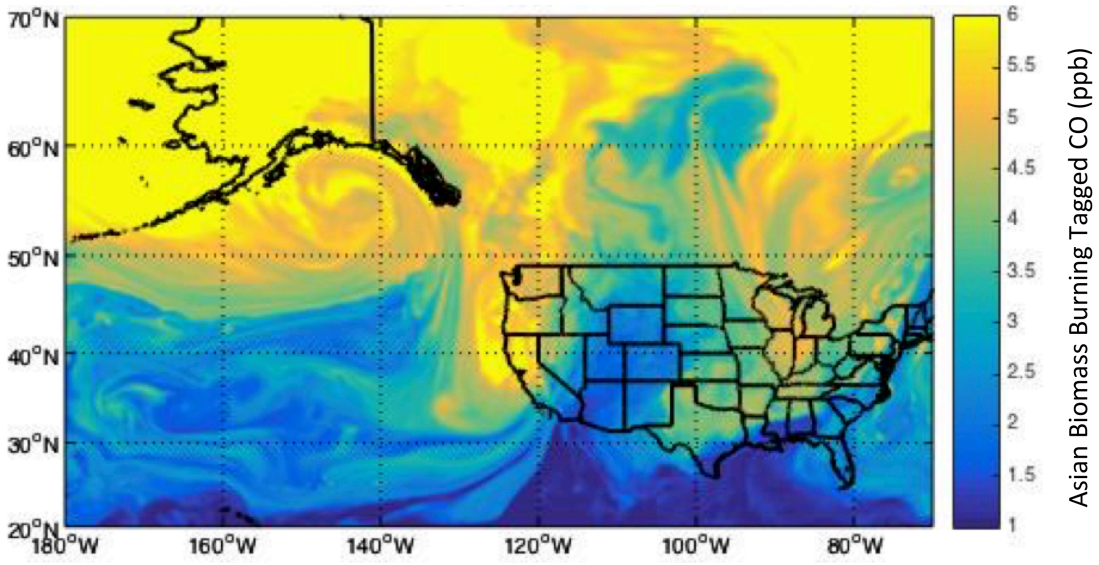

Figure 12: GEOS-5 CO biomass burning tagged tracers at 300mb from Europe & Asia on 22 September 2013 at 00UTC.

GEOS-5 CO biomass burning tagged tracers from Europe/Asia simulated some influence behind the cold front on 21 September 2013 as shown in Figure 12. The tagged tracers showed CO of a few ppbv from European/Asian biomass burning reaching locations behind the cold front across Tennessee and Arkansas, which is in agreement with in-situ observations from Figure 7a that show very small variability in CO for the HOLW regions.

Aircraft measurements showed two HOLW regions behind the cold front on 21 September 2013. The air in the HOLW regions may have origins in the biomass burning regions in eastern China as the long lifetime biomass burning tracer HCN is elevated, whereas shorter lifetime tracers such as C_2H_4 and CH_2O showed no enhancements in these regions. Dynamics behind the cold front and H_2O in-situ observations suggest that the air was likely in the UT/LS before being transported into the mid-troposphere.

September 23, 2013

Meteorological Conditions

Only days after the 21 September case study, another cold frontal passage occurred in the central United States. Ahead of the front, most regions were experiencing near normal temperatures despite southerly flow due to the cool air still residing in the air behind the previous front. On 22 September the front was moving through the eastern Rockies and beginning to push into the central Plains as shown in Figure 13. The front continued to push east moving into the regions of the DC-8 flight path on 23 September. The DC-8 flew through the front in central Oklahoma sampling the tropopause fold as it passed through this region. This front was much weaker than the front on 21 September as strongest winds in the jet streak were only ~36m/s, whereas the front on 21 September had winds greater than 77m/s in the jet streak.

Given that the air mass was stable ahead of the front due to the relatively cool surface temperatures, there was very little precipitation associated with this front.

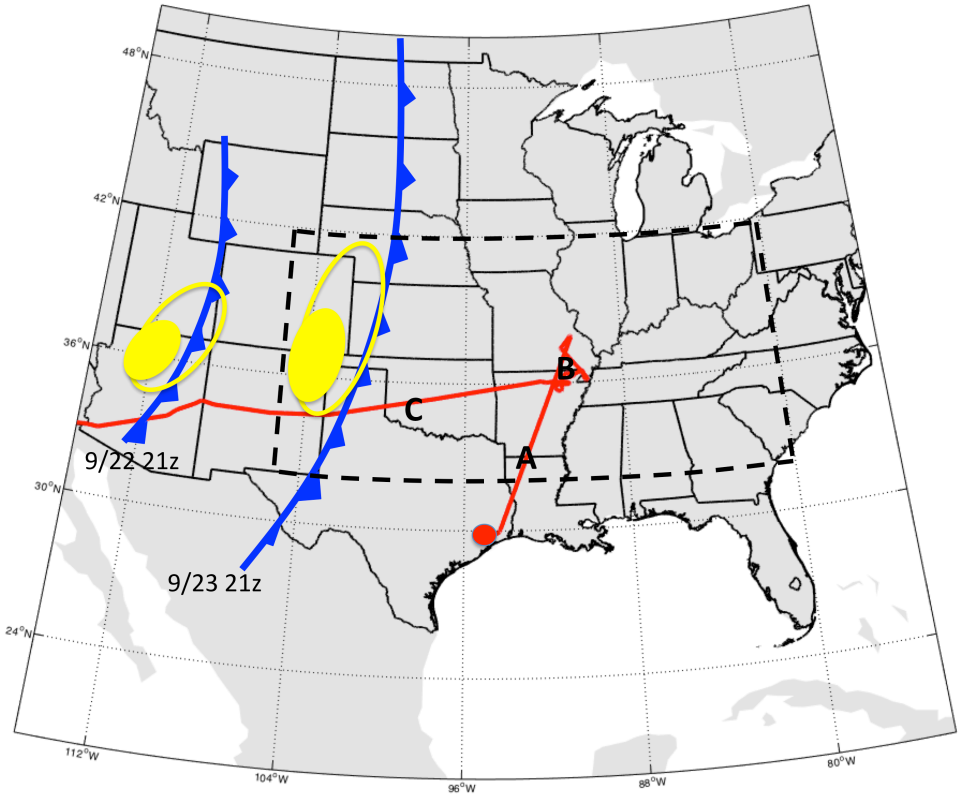

Figure 13: Map shows location of the cold front as it pushes through the southeast United States and flight path of DC-8 on 23 September 2013 in red line with letters representing different legs of the flight. Red dot is location where flight originated. Yellow circle represents region of jet streak with inner region representing area where stratospheric intrusion is likely.

Aircraft Observations/Mixing Line Analysis

The DC-8 flew across portions of the United States on 23 September 2013 with several goals on the final flight of the campaign. Early portions of this flight denoted by A and B on Figure 13 across the southeast United States sampled isoprene emissions and localized burning in the Ozarks. As the aircraft continued flying westward, it intersected a weak cold front in central Oklahoma around 2050UTC. Once passing west of the cold front, two HOLW layers were observed (~2120UTC and 2200UTC on Figure 14). As with the cold front on 21 September, CO was constant through this region at around 60ppbv while both O_3 and HCN (90-100ppbv and 400pptv respectively) were enhanced above background values and highly correlated (r^2 of 0.75).

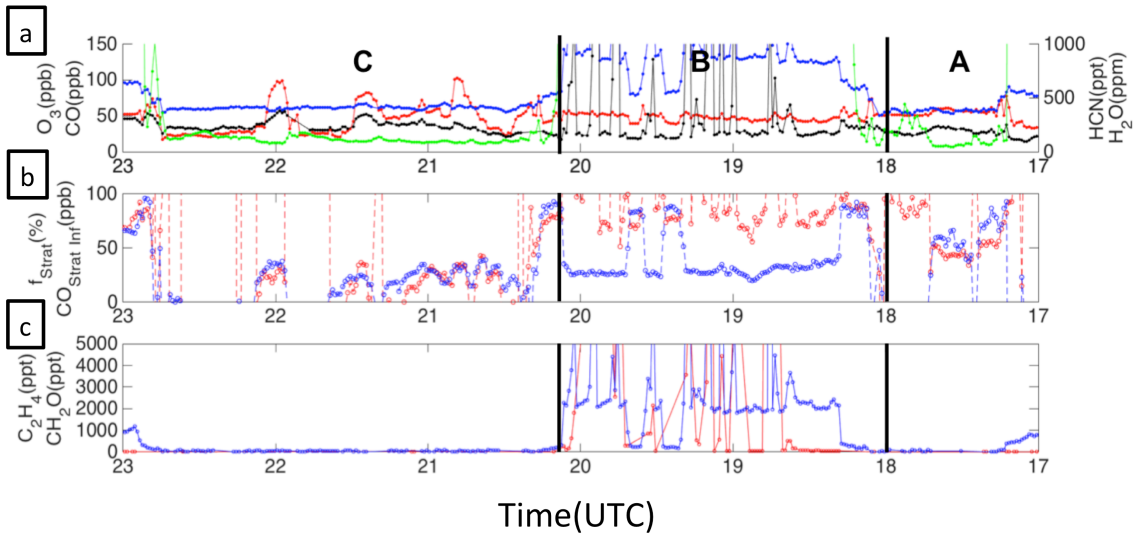

Figure 14: In-situ observations and model simulations on 23 September 2013. a) In-situ aircraft observations of O_3 (red), CO (blue), H_2O (green), and HCN (black); b) Mixing line analysis showing f_{strat} (in blue) and $CO_{Strat\ Inf}$ (in red) c) In-situ aircraft observations of C_2H_4 (blue) and CH_2O (red)

A mixing line analysis for this flight showed much less influence of stratospheric air than on 21 September (around 40%). The corresponding inferred stratospheric CO, however, was much lower at around 40ppbv due to f_{strat} being very low. The much

weaker stratospheric influence from the mixing line analysis could have been due to the fact that this front was weaker; the vertical transport into the troposphere was likely weaker as well.

The DIAL O_3 profile shows two different layers of elevated O_3 behind the front, one around 400-600mb and another around 250mb. Aircraft observations in the 400-600mb layer confirm it as a HOLW (Figure 14a portion C) since H_2O is ~180ppmv and O_3 is ~75ppbv at 475mb. Given the HOLW characteristic of this layer, it likely was brought down from the UT/LS, but resided in the lower troposphere for several days and mixed with tropospheric air as background UT/LS H_2O is ~20-150ppmv. This layer resides just along the top of the boundary layer but does not become entrained into the boundary layer. The elevated O_3 layer at 250mb is the layer of interest that may be a mixture of UT/LS air and may be mixed with biomass burning.

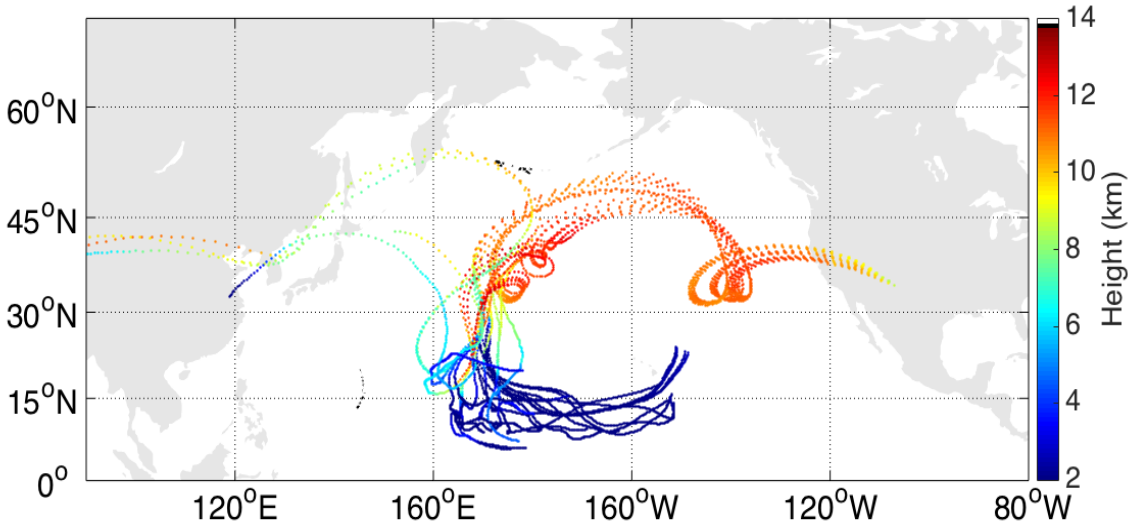

Figure 15: NOAA Hysplit back trajectories initialized at 2200UTC on 23 September 2013 for 34.40N, -107.09W at 300mb.

NOAA HYSPLIT back trajectory ensembles show a variety of origins for the air in these two layers (Figure 15). One region is in the central Pacific where Hysplit lofts

the air due to intense convection associated with a tropical cyclone in the central Pacific. Three ensembles, however, as with the 21 September case study, trace the air back to eastern China where widespread biomass burning is occurring. While this leads to large uncertainty due to the convection in most ensemble members, the combination of a few members originating in China long with in-situ observations show some of the air possibly did come from Asian biomass burning.

GEOS-5/CMAQ Model Simulations

Model simulations compared to DIAL O_3 observations show very similar structure in the elevated O_3 layers for this case study as shown in Figure 16. GEOS-5 shows stratospheric influence in the elevated O_3 layer in the mid-troposphere from 2030UTC to 2300UTC as well as the layer around 250mb (Figures 16a & 16b). The lower layer in GEOS-5 shows a smaller percentage of stratospheric air, which agrees with the analysis from in-situ observations that this air originated in the UT/LS a few days earlier.

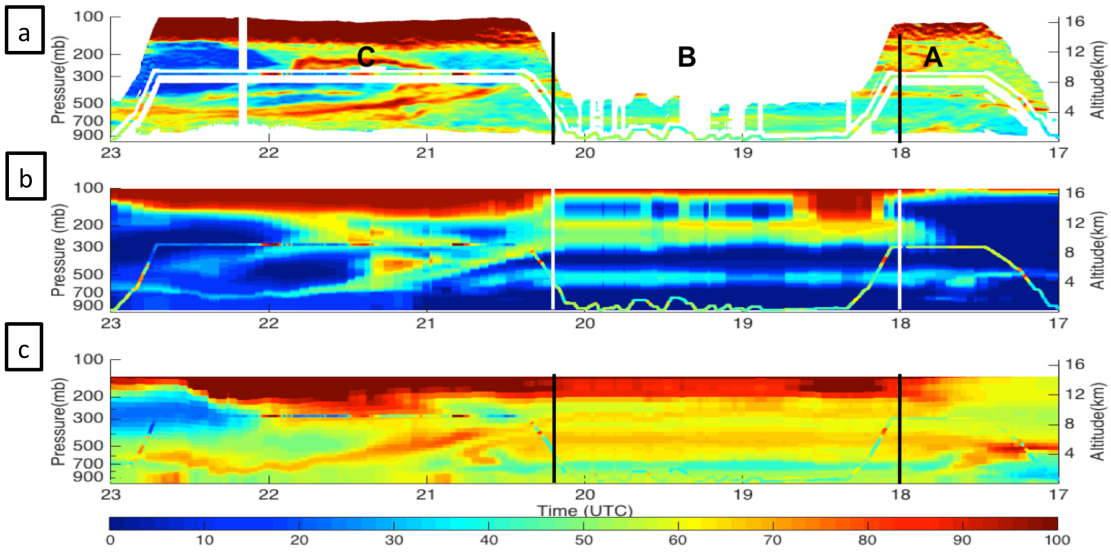

Figure 16: LiDAR observations and model simulations with in-situ aircraft profiles overlaid in each profile for 23 September 2013. a) DIAL LiDAR O_3 profile; b) GEOS-5 stratospheric tracer profile; c) CMAQ O_3 profile

CMAQ shows the same layers of enhanced O_3 that are measured with the DIAL instrument and simulated with GEOS-5. CMAQ simulated O_3 of ~90ppbv for both layers which compares well with DIAL O_3 of ~70-90ppbv (Figures 16a and 16c). Outside the enhanced O_3 layers CMAQ overestimates background tropospheric O_3 as it models much of the tropospheric O_3 greater than 40ppbv whereas in-situ O_3 measurements and DIAL O_3 measurements were below 30ppbv in most of these regions.

GEOS-5 CO biomass burning tagged tracers from Europe/Asia, as shown in Figure 12, show several ppbv of CO behind the front as it moves inland along the west coast of the United States on 22 September 2013. This compares well with in-situ observations that show very small variability in CO of a few ppbv but some Asian biomass burning influence due to enhanced HCN measurements (Figure 14a).

In-situ observations show two HOLW regions behind the cold front on 23 September 2013. Similarly to the case on 21 September 2013, in-situ measurements of enhanced HCN show possible biomass burning origin. While most HYSPLIT trajectory ensembles initialized in these regions are lofted in convection in the central Pacific, a few do trace back to eastern China where biomass burning was occurring. As with the case on 21 September, both in-situ observations of H_2O and dynamic meteorology suggest that the HOLW layers were in the UT/LS and brought down to the mid-troposphere through a stratospheric intrusion. DIAL observations show that HOLW air from the UT/LS mixes down to the top of the boundary layer without entraining into the boundary layer for this case study.

IV. Conclusions

Previous research has shown large O_3 enhancements due to biomass burning after approximately 10 days. Here we show that in the central United States the enhancement can occur much quicker with O_3 of 120ppbv being produced within three days of the biomass burning emission. The quicker O_3 enhancement in this region could be either caused by the rapid dispersion of smoke allowing for increased absorption of solar radiation or mixing with local pollutant sources leading to very high concentrations of O_3 precursors.

We present case studies of several HOLW regions behind cold front passages in the central and southeastern United States. A mixing line analysis for these layers show possible mixed UT/LS air with possible biomass burning influences. The mixing line analysis does show conclusive results in the continental United States due to the difficulty in determining background H_2O in areas that see highly variable H_2O. These regions have characteristics of aged biomass burning with enhanced levels of HCN, and may have been transported from biomass burning regions in eastern Asia based on back trajectories from NOAA's HYSPLIT model. Given the dynamics and low H_2O in these layers, they likely were transported from the UT/LS by a stratospheric intrusion.

GEOS-5 global model and CMAQ regional air quality model reproduce the structure of enhanced O_3 layers associated with HOLW regions. CMAQ does not correctly simulate the background tropospheric O_3, but rather overestimates O_3 by as much as 20-30ppbv.

Ozone from the UT/LS had no impact on air quality during the campaign period. DIAL measured enhanced O_3 along the top of the PBL but not entraining into the PBL. Ground based measurements from Penn State's NATIVE trailer did not show any HOLW layers reaching the surface at Smith Point, TX.

References:

Anderson DC, Nicely JM, Salawitch RJ, et al. A pervasive role for biomass burning in tropical high ozone/low water structures. *Nature Communications*. 2016;7:10267. doi:10.1038/ncomms10267.

Alvarado, M. J., Logan, J. A., Mao, J., Apel E, Riemer, D., Blake, D., Cohen, R. C., Min, K.-E., Perring, A. E., Browne, E.C., Wooldridge, P. J., Diskin, G. S., Sachse, G.W., Fuelberg, H., Sessions, W. R., Harrigan, D. L., Huey, G., Liao, J., Case-Hanks, A., Jimenez, J. L., Cubison, M. J., Vay, S. A., Weinheimer, A. J., Knapp, D. J., Montzka, D. D., Flocke, F. M., Pollack, I. B., Wennberg, P. O., Kurten, A., Crounse, J., St. Clair, J. M., Wisthaler, A., Mikoviny, T., Yantosca, R. M., Carouge, C. C., and Le Sager, P (2010), Nitrogen oxides and PAN in plumes from boreal fires during ARCTAS-B and their impact on ozone: an integrated analysis of aircraft and satellite observations, Atmos. Chem. Phys., 10, 9739–9760.

Canty, T.P., L. Hembeck, T.P. Vinciguerra, D.C. Anderson, D.L. Goldberg, S.F. Carpenter, D.J. Allen, C.P. Loughner, R.J. Salawitch, and R.R. Dickerson (2015), Ozone and NOx chemistry in the eastern US: Evaluation of CMAQ/CB05 with satellite (OMI) data, Atmospheric Chemistry and Physics, 15, 10965-10982.

Cooper, O., Forster, C., Parrish, D., Dunlea, E., Hübler, G., Fehsenfeld, F., Holloway, J., Oltmans, S., Johnson, B., Wimmers, A., and Horowitz, L. (2004), On the life cycle of a stratospheric intrusion and its dispersion into polluted warm conveyor belts, J. Geophys. Res., 109, D23S09, doi:10.1029/2003JD004006.

Danielsen, E. F. (1968), Stratospheric-tropospheric exchange based on radioactivity, ozone and potential vorticity, J. Atmos. Sci., 25, 502 – 518.

Holmen, A., Blomqvist, J., Frindberg, H., Johnelius, Y., Eriksson, N. E., Henricson, K. A., et al. (1997). Frequency of patients with acute asthma in relation to ozone, nitrogen dioxide, other pollutants of ambient air and meteorological observations. International Archives of Occupational and Environmental Health, 69, 317–322.

Jolleys, M, H. Coe, G. McFiggans, G. Capes, J. Allan, J. Crosier, P. Williams, G. Allen, K. Bower, Jose. Jimenez, L. Russell, M. Grutter, and D. Baumgardner (2012), Characterizing the Aging of Biomass Burning Organic Aerosol by Use of Mixing Ratios: A Meta-analysis of Four Regions. Enviornmental Science & Technology. Doi:10.1021/es302386v.

Lin, M., Fiore, A.M., Cooper, O.R., Horowitz, L.W., Langford, A.O., Levy II, H., Johnson, B.J., Naik, V., Oltmans, S.J., Senff, C.J. (2012), Springtime high surface ozone events over the western United States: Quantifying the role of stratospheric intrusions. J. Geophys. Res. 117, D00V22, doi:10.1029/2012JD018151.

Lippmvann M. (1989). Health effects of ozone: A critical review. J. Air Pollution Control Assoc 39: 672-695.

Martins, D., Stauffer R., Thompson, A., Knepp, T., Pippin, M. (2012), Surface ozone at a coastal suburban site in 2009 and 2010: Relationships to chemical and meteorologica processes. J. Geophys. Res.. doi: 10.1029/2011JD016828.

May, R. D. (1998), Open-path, near-infrared tunable diode laser spectrometer for atmospheric measurements of H_2O, J. Geophys. Res., **103**(D15),19,161–19,172, doi:10.1029/98JD01678.

Oltmans, S. J., et al. (2010), Enhanced ozone over western North America from biomass burning in Eurasia during April 2008 as seen in surface and profile observations, Atmos. Environ., 44, 4497–4509, doi:10.1016/ j.atmosenv.2010.07.004.

Parrington, M., Palmer, P. I., Henze, D. K., Tarasick, D. W., Hyer, E. J., Owen, R. C., Helmig, D., Clerbaux, C., Bowman, K. W., Deeter, M. N., Barratt, E. M., Coheur, P.-F., Hurtmans, D., Jiang, Z., George, M., and Worden, J. R. (2012), The influence of boreal biomass burning emissions on the distribution of tropospheric ozone over North America and the North Atlantic during 2010, Atmos. Chem. Phys., 12, 2077–2098, doi:10.5194/acp-12-2077- 2012.

Parrish, D. D., J. S. Holloway, R. Jakoubek, M. Trainer, T. B. Ryerson, G. Hubler, F. C. Fehsenfeld, J. L. Moody, and O. R. Cooper (2000), Mixing of anthropogenic pollution with stratospheric ozone: A case study from the North Atlantic wintertime troposphere, J. Geophys. Res., 105, 24,363 – 24,374.

Podolske, J., Sachse, G., and Diskin, G.. (2003), Calibration and data retrieval algorithms for the NASA Langley/Ames Diode Laser Hygrometer for the NASA Transport and Chemical Evolution Over the Pacific (TRACE-P) mission. J. Geophys. Res. 108: doi: 10.1029/2002JD003156.

Ryerson, T, Trainer, M., Angevine, W., Brock, C., Dissly, R., Fehsenfeld, F., Frost, G., Goldan, P., Holloway, J., Hubley, G., Jakoubek, R., Kuster, W., Neuman, J., Nicks, D., Parrish, D., Roberts, J., Sueper, D., Atlas, E., Donnelly, S., Flocke, F., Fried, A., Potter, W., Schauffler, S., Stroud, V., Weinheimer, A., Wert, B., Wiedinmyer, C., Alvarez, R., Banta, R., Darby, L., and Senff, C. (2003), Effect of petrochemical

industrial emissions of reactive alkenes and NO_x on tropospheric ozne formation in Houston, Texas. J. Geophys. Res. 108: doi: 10.1029/2002JD003070.

Sachse, G., Hill, G., Wade, L., and Perry, M. (1987), Fast-response high-precision carbon monoxide sensor using a tunable diode laser absorprtion technique. J. Geophys. Res. 92: doi: 10.1029/JD092iD02p02071.

Sahu, L. K., Kondo, Y., Moteki, N., Takegawa, N., Zhao, Y., Cubison, M. J., Jimenez, L. J., Vay, S., Diskin, G. S., Wisthaler, A., Mikoviny, T., Huey, L. G., Weinheimer, A. J. J., and Knapp, D., (2012), Emission characteristics of black carbon in anthropogenic and biomass burning plumes over California during ARCTAS-CARB 2008, J. Geophys. Res., v. 117, p. D16302, pp. 1-20, doi:10.1029/2011JD017401.

Schroeder D. M., Blankenship D. D., Young D. A., Quartini E. (2014), Evidence for elevated and spatially variable geothermal flux beneath the West Antarctic Ice Sheet.Proceedings of the National Academy of Sciences of the United States of America. 111(25):9070-9072. doi:10.1073/pnas.1405184111.

Shapiro, M. A. (1980), Turbulent mixing within tropopause folds as a mechanism for the exchange of chemical constituents between the stratosphere and troposphere, J. Atmos. Sci., 37, 994 – 1004.

Shine, K. (2001) Atmospheric Ozone and Climate Change, Ozone: Science & Engineering, 23:6, 429-435, DOI: 10.1080/01919510108962026

Stohl, A., et al. (2003), Stratosphere-troposphere exchange: A review, and what we have learned form STACCATO, J. Geophys. Res., 108(D12), 8516, doi:10.1029/2002JD002490.

Thompson, A.M., Stone, J. B., Witte, J.C., Miller, S.C., Oltmans, S.J., Ross, K. L., Kucsera, T.L., Merrill, J.T., Forbes, G., Tarasick, D.W., Joseph, E., Schmidlin, F.J., McMillan, W.W., Warner, J., Hintsa, E.J., Johnson, J.E. (2007), Intercontinental Transport Experiment Ozonesonde Network Study (IONS, 2004): 2. Tropospheric Ozone Budgets and Variability over Northeastern North America, J. Geophys. Res., 112, D12S13, doi: 10.1029/2006JD007670.

Thompson, A., Witte, J., Smit, H., Oltmans, S., Johnson, B., Kirchhoff, V., and Schmidlin, F. (2007a), Southern Hemisphere Additional Ozonesondes (SHADOZ) 1998-2004 tropical ozone climatology: 3. Instrumentation, station-to-station variability, and evaluation with simulated flight profiles. J. Geophys. Res.. doi: 10.1029/2005JD007042.

Thompson, A., Stone, J., Witte, J., Miller, S., Oltmans, S., Kucsera, T., Ross, K., Pickering, K., Merrill, Forbes, G., Tarasick, D., Joseph, E., Schmidlin, F., McMillan, W., Warner, J., Hintsa, E., Johnson, J. (2007), Intercontinental Chemical Transport Experiment Ozonesonde Network Study (IONS) 2004: 2. Tropospheric ozone budgets and variability over northeastern North America. J. Geophys. Res., Doi: 10.1029/2006JD007441.

Toon, O., Maring, H., Dibb, J., Ferarre, R., Jacob, D., Jensen, E., Luo, Z., Mace, G., Pan, L., Pfister, L., Rosenlof, K., Redemann, J., Reid, J., Singh, H., Thompson, A., Yokelson, R., Minnis, P., Chen, G., Jucks, K., Pszenny, A. (2016), Planning, implementation and scientific goals of the Studies of Emissions and Atmospheric Composition, Clouds, and Climate Coupling by Regional Surveys (SEAC4RS) field mission. J. Geophys. Res.. Doi: 10.1002/2015JD024297.

Unger, N., Shindell, D., Koch, D., and Streets, D. (2006), Cross Influences of Ozone and Sulfate Precursor Emissions Changes on Air Qaulity and Climate. PNAS. doi: 10.1073/pnas.0508769103

Vay, S.A., Anderson, B.E., Jensen, E.J., Sachse, G.W., Ovarlez, J., Gregory, G.L., Nolf, S.R., Podolske, J.R., Slate, T.A., and Sorenson, C.E. (2000), Tropospheric water vapor measurements over the North Atlantic during the Subsonic Assessment Ozone and Nitrogen Oxide Experiment (SONEX). J. Geophys. Res., 105, 3745-3756.

Viggiano, A. A., Hunton, D.E., Miller, T.M., and Ballenthin, J.O. (2000), In situ measurements of hydrogen cyanide in the upper troposphere/lower stratosphere during Arctic spring. J. Geophys. Res., 108(D5), 8304, doi:10.1029/2001JD001033, 2003.

Washenfelder, R. A., Trainer, M., Frost, G. J., Ryerson, T. B., Atlas, E. L., de Gouw, J. A., Flocke, F. M., Fried, A., Holloway, J. S., Parrish, D. D., Peischl, J., Richter, D., Schauffler, S. M., Walega, J. G., Warneke, C., Weibring, P., and Zheng, W. (2010), Characterization of NOx, SO2, ethene, and propene from industrial emission sources in Houston, Texas, J. Geophys. Res., 115, D16311, 10.1029/2009jd013645.

Weibring, P., Richter, D., Walega, J.G., Rippe, L., and Fried, A. (2010), Difference Frequency Generation Spectrometer for Simultaneous Multispecies Detection, Optics Express, 18 (26), 27,670 – 27,681.